Reviews

Nitrogen-15 and Oxygen-17 NMR Spectroscopy of Silicates and Nitrogen Ceramics

Robin K. Harris* and Matthew J. Leach†

Department of Chemistry, University of Durham, South Road, Durham DH1 3LE, U.K.

Derek P. Thompson

Department of Mechanical, Materials and Manufacturing Engineering, The University, Newcastle upon Tyne NE1 7RU, U.K.

Received November 18, 1991. Revised Manuscript Received January 30, 1992

The value of nitrogen-15 and oxygen-17 NMR for the chemical structure determination of ceramic compounds is discussed, and available data are reviewed. Ranges of chemical shifts for different coordination types are deduced. A substantial number of new results for materials of the sialon type are presented. Relationships with crystallography are highlighted. In the case of ^{17}O the additional problems inherent in dealing with a quadrupolar nucleus are mentioned.

Introduction

Silicon-29[1–13] and aluminum-27[1,5,8,14,15] NMR have provided a great deal of information on the structures of silicates and nitrogen ceramics (or "sialons"—compounds involving the elements silicon, aluminum, oxygen, and nitrogen[16,17]). The short-range nature of the factors influencing NMR spectra means that in partially covalent materials such as silicates and nitrogen ceramics, chemical shifts are most sensitive to nearest-neighbor coordination. This implies that to gain the most information on oxygen and nitrogen environments in these materials, it is necessary to observe these nuclei directly. Attention has therefore recently turned to this matter, generally but not always using isotopic enrichment. The aim of this paper is to review these studies, including a substantial number of new results obtained in our laboratories. The scope of this article has been confined to studies on oxides, silicates, and silicon-containing nitrogen ceramics, although some other relevant reports will also be considered. Throughout this review, site occupation is described in terms of the standard Wyckoff nomenclature, as given in the International Tables for X-ray Crystallography.

Experimental Section

Nitrogen-15-containing phases were prepared from α-$Si_3{}^{15}N_4$ by standard methods.[18,19] α-$Si_3{}^{15}N_4$ was prepared as described previously.[20] Samples enriched in ^{17}O were prepared from $Si^{17}O_2$ and $Mg^{17}O$, using standard methods,[18,19] with $Si^{17}O_2$ obtained by hydrolysis of $SiCl_4$ with $H_2{}^{17}O$ (22% ^{17}O; Amersham) as described previously,[21] and $Mg^{17}O$ by hydrolysis of $Mg(C_2H_5)_2$ with $H_2{}^{17}O$.[19] In all cases, sample purity was checked by powder XRD.

Nitrogen-15 and oxygen-17 MAS NMR spectra were obtained at 30.4 and 40.7 MHz, respectively, by using a Varian VXR300 spectrometer. Some additional oxygen-17 NMR spectra were obtained at 27.1 MHz by using a Bruker CXP200 spectrometer. Spectrometer operating conditions were as given in the figure captions. Samples were packed in zirconia or alumina rotors and spun at 3–10 kHz during acquisition. Nitrogen-15 recycle delays were typically long because of the high relaxation times found.[20] Full details of how pulse sequence parameters were chosen are given in ref 19. Nitrogen-15 chemical shifts are quoted relative to the ammonium resonance of solid NH_4NO_3. (See refs. 19 and 22 for a more complete discussion on referencing of ^{15}N spectra.) Quadrupolar effects mean that ^{17}O relaxation times are substantially less than those for ^{15}N, so that recycle delays of only a second or so suffice in the former case. Oxygen-17 chemical

* To whom correspondence should be addressed.

† Present address: Unilever Research, Quarry Road East, Bebington, Wirral L63 3JW, U.K.

(1) Engelhardt, G.; Michel, D. *High Resolution Solid-State NMR of Silicates and Zeolites*; Wiley: Chichester, U.K. 1987; Chapter 4.
(2) Mägi, M.; Lippmaa, E.; Samoson, A.; Engelhardt, G.; Grimmer, A.-R. *J. Phys. Chem.* **1984**, *88*, 1518.
(3) Janes, N.; Oldfield, E. *J. Am. Chem. Soc.* **1985**, *107*, 6769.
(4) Sherriff, B. L.; Grundy, H. D. *Nature* **1988**, *332*, 819.
(5) Klinowski, J.; Thomas, J. M.; Thompson, D. P.; Korgul, P.; Jack, K. H.; Fyfe, C. A.; Gobbi, G. C. *Polyhedron* **1984**, *3*, 1267.
(6) Dupree, R.; Lewis, M. H.; Leng-Ward, G.; Williams, D. S. *J. Mater. Sci. Lett.* **1985**, *4*, 393.
(7) Dupree, R.; Lewis, M. H.; Smith, M. E. *J. Am. Chem. Soc.* **1988**, *110*, 1083.
(8) Dupree, R.; Lewis, M. H.; Smith, M. E. *J. Am. Chem. Soc.* **1989**, *111*, 5125.
(9) Harris, R. K.; Leach, M. J.; Thompson, D. P. *Chem. Mater.* **1989**, *1*, 336.
(10) Leach, M. J.; Harris, R. K.; Thompson, D. P. *Euro-Ceramics*; de With, G., Terpstra, R. A., Metselaar, R., Eds.; Elsevier: London, 1990, Vol. 2, 140.
(11) Aujla, R. S.; Leng-Ward, G.; Lewis, M. H.; Seymour, E. F. W.; Styles, G. A.; West, G. W. *Philos. Mag. B* **1986**, *54*, L51.
(12) Carduner, K. R.; Blackwell, C. S.; Hammond, W. B.; Reidinger, F.; Hatfield, G. R. *J. Am. Chem. Soc.* **1990**, *112*, 4676.
(13) Hatfield, G. R.; Li, B.; Hammond, W. B.; Reidinger, F.; Yamanis, J. *J. Mater. Sci.* **1990**, *25*, 4032.
(14) Lippmaa, E.; Samoson, A.; Mägi, M. *J. Am. Chem. Soc.* **1986**, *108*, 1730.
(15) Dupree, R.; Lewis, M. H.; Smith, M. E. *J. Appl. Crystallogr.* **1988**, *21*, 109.
(16) Jack, K. H. *Nitrogen Ceramics*; Riley, F. L., Ed.; NATO ASI 1977; Vol. E 23, pp. 109–128.
(17) Jack, K. H. *Sci. Ceram.* **1981**, *11*, 125.
(18) Rae, A. W. J. M. Ph.D. Thesis, University of Newcastle upon Tyne, 1976.
(19) Leach, M. J. Ph.D. Thesis, University of Durham, 1990.
(20) Harris, R. K.; Leach, M. J.; Thompson, D. P. *Chem. Mater.* **1990**, *2*, 320.
(21) Abys, J. A.; Barnes, D. M.; Feller, S.; Rouse, G. B.; Risen Jnr., W. M. *Mater. Res. Bull.* **1980**, *15*, 1581.
(22) Mason, J. *Multinuclear NMR*; Mason, J., Ed.; Plenum, New York, 1987; p 335.

0897-4756/92/2804-0260$03.00/0

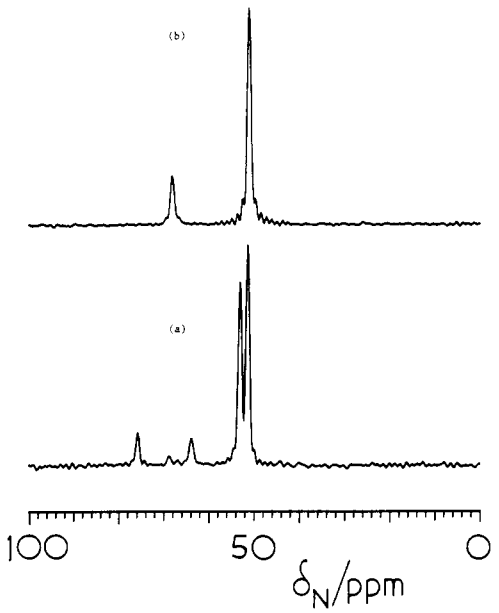

Figure 1. Nitrogen-15 MAS spectra at 30.4 MHz of (a) α-$Si_3{}^{15}N_4$ and (b) β-$Si_3{}^{15}N_4$. Spectrometer conditions: spin rate 4.40 kHz, pulse angle 90° (for a) and 10° (for b); number of transients 11 (for a) and 192 (for b); recycle delay 3600 s (for a) and 300 s (for b). Reprinted, with permission, from ref 20.

shifts are quoted relative to the signal from H_2O. In each case the high-frequency-positive convention is used.

Nitrogen-15 NMR. General. Nitrogen is present in natural abundance as 99.6% ^{14}N ($I = 1$) and 0.4% ^{15}N ($I = {}^1/_2$). There have been a few reports of ^{14}N studies on inorganic solids,[23] but ^{15}N is far preferable for the vast majority of systems once problems associated with the low natural abundance have been overcome.

There have been relatively few studies of ^{15}N MAS NMR in inorganic solids, principally because of the desirability of isotopic enrichment, which is expensive and/or time-consuming. Natural abundance spectra have generally been acquired with the aid of cross-polarization (CP) from protons.[24,25] To study ceramic phases, isotopic enrichment is generally required (but see Marshall et al.[26]) because CP cannot be used. A further problem for ^{15}N NMR of ceramics is that spin–lattice relaxation times can be substantial (because of the rigidity of the structures and the lack of protons) and are generally not known, so that substantial relaxation delays are usually necessary between pulses, resulting in inefficient spectrometer usage.

Harris et al.[20] have described the ^{15}N MAS NMR spectra of ^{15}N-enriched α- and β-Si_3N_4. Both phases possess an infinite covalent structure in which nitrogen is always bonded to three silicon atoms. We designate this arrangement as an [NSi_3] environment, the square brackets being used to denote a structural unit consisting of the central atom of interest plus nearest neighbours. The nitrogen sites in α- and β-Si_3N_4 are geometrically very similar, but not identical. The spectra (Figure 1) of these compounds show chemical shifts of 50–75 ppm in agreement with the planar [NSi_3] environment of the nitrogen atoms.[27,28] The two peaks in β-Si_3N_4 (space group $P6_3$), present in the intensity ratio 3:1, are consistent with the eight nitrogen atoms in the unit cell occupying 6(c) and 2(b) sites. In α-Si_3N_4 (space group $P3_1c$), the doubled c repeat (compared with β-Si_3N_4) gives rise to 16 nitrogen atoms per cell, occupying 2 sets of 6(c) plus single sets of 2(b) and 2(a) positions, again consistent with the four NMR peaks in intensity ratios 3:3:1:1. The related phase $Si_2{}^{15}N_2O$ gives

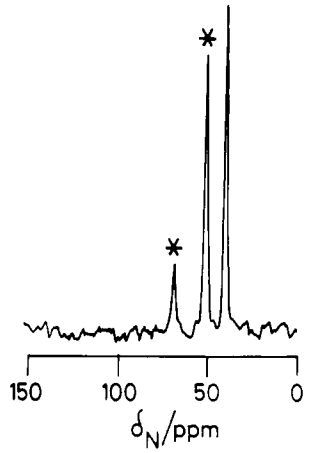

Figure 2. Nitrogen-15 MAS spectrum at 30.4 MHz of $Si_2{}^{15}N_2O$. Peaks marked by an asterisk rise from impurity β-Si_3N_4. Spectrometer conditions: spin rate 3.03 kHz; pulse angle 11°; number of transients 184; recycle delay 120 s.

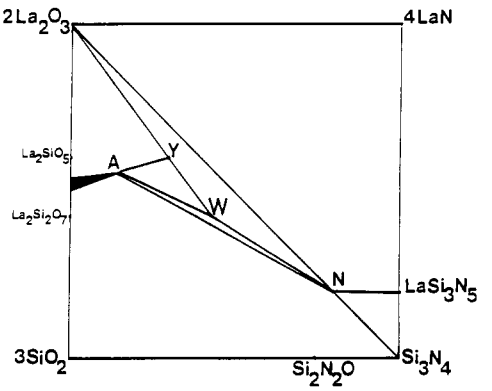

Figure 3. Phase diagram for the La–Si–O–N system at 1550 °C. The lines represent known relationships involving phases A, Y, W, and N only. The black area indicates a range of homogeneity.

Table I. ^{15}N MAS NMR Data for ^{15}N-Enriched La Sialons

phase	δ_N/ppm	fwhh[c]/Hz	intensity
"new phase", $La_3Si_8O_4N_{11}$	~64	500	4
	~126	1400	7
La–N–wollastonite, $LaSiO_2N$	154.9	330	
La–N–YAM, $La_4Si_2O_7N_2$	*a*		
$LaSi_3N_5$	51.4[b]	60	0.2
	71.3	175	3
	110–160	1500	4
Al-containing "new"	50.1[b]	100	
$La_3Si_6Al_2O_6N_9$	66.9	500	2
	130	1400	3

[a] No signal observed. [b] Signal from β-Si_3N_4. [c] Full width at half-height.

a similar chemical shift (40.3 ppm) corresponding to a single [NSi_3] environment (Figure 2). These results are in agreement with those of Turner et al.,[29] who reported the spectrum of a mixed $Si_2{}^{15}N_2O/Si_3{}^{15}N_4$ sample, although their assignment was not totally correct. They suspected that the second ^{15}N peak for β-Si_3N_4 was due to metal nitride impurity from the furnace lining, but they did not consider that β-Si_3N_4 should itself give two ^{15}N peaks.

Bunker et al.[30] have studied a series of ^{15}N-enriched sodium phosphate glasses. Nitrogen in [NP_3] and [NP_2] environments can readily be distinguished; the former environment gives δ_N in the range 88–93 ppm, and the latter in the range 55–63 ppm.

La–Si–O–N and Related Systems. The phases present in the La–Si–O–N system have been described elsewhere.[8,9,31,32] The

(23) Merwin, L. H. Ph.D. Thesis, University of Durham, 1987.
(24) Mason, J.; Mingos, D. M. P.; Schaefer, J.; Sherman, D.; Stejskal, E. O. *J. Chem. Soc., Chem. Commun.* **1985**, 444.
(25) Harris, R. K.; Merwin, L. H.; Hägele, G. *Magn. Reson. Chem.* **1989**, *27*, 470.
(26) Marshall, G. L.; Harris, R. K.; Apperley, D. C.; Yeung, R. R. *Sci. Ceram.* **1987**, *14*, 347.
(27) Grün, R. *Acta Crystallogr.* **1979**, *B35*, 800.
(28) Kato, K.; Inoue, Z.; Kijima, K.; Yamane, T.; Kawada, J. *J. Am. Ceram. Soc.* **1975**, *58*, 90.
(29) Turner, G. L.; Kirkpatrick, R. J.; Risbud, S. H.; Oldfield E. *Am. Ceram. Soc. Bull.* **1987**, *66*, 656.
(30) Bunker, B. C.; Tallant, D. R.; Balfe, C. A.; Kirkpatrick, R. J.; Turner, G. L.; Reidmeyer, M. R. *J. Am. Ceram. Soc.* **1987**, *70*, 675.

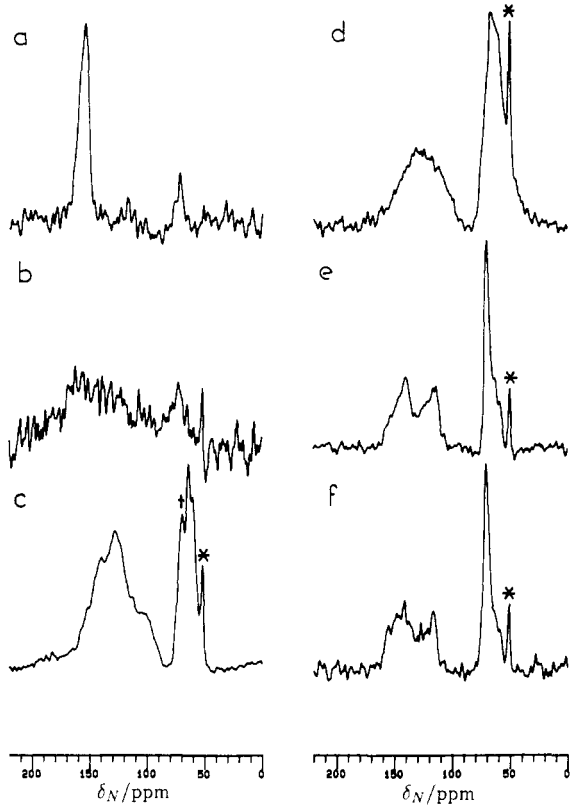

Figure 4. Nitrogen-15 MAS spectra at 30.4 MHz for isotopically enriched ceramics: (a) La–N–wollastonite, $LaSiO_2N$, (b) La–N–YAM, $La_4Si_2O_7N_2$, (c) "new phase", $La_3Si_8O_4N_{11}$, (d) "La–Al new phase", $La_3Si_6Al_2O_6N_9$, (e) $LaSi_3N_5$, (f) $LaSi_3N_5$ (second sample). The peaks marked by asterisks probably arise from impurity α-Si_3N_4, as may (partly) the one in c marked with a dagger. Spectrometer conditions (each in order a to f): spin rate 3.75, 4.02, 3.75, 3.15, 3.00, 3.28 kHz; pulse angle 90°, 70°, 23°, 17°, 30°, 17°; number of transients 10, 31, 300, 141, 214, 219; recycle delay 3600, 3600, 300, 300, 300, 300 s.

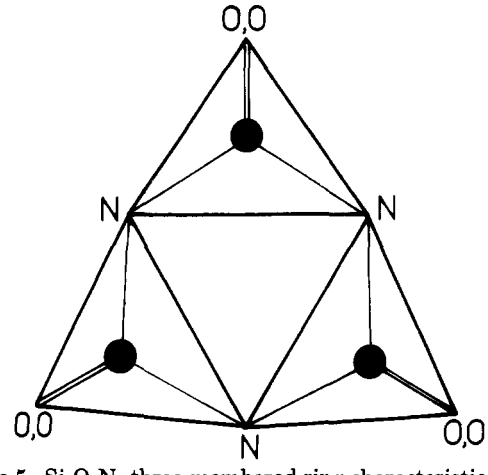

Figure 5. $Si_3O_6N_3$ three-membered ring characteristic of N–α-wollastonite structures, showing the bridging site occupied by nitrogen and nonbridging sites occupied by oxygen.

phase diagram for this system is shown in Figure 3. Nitrogen-15 MAS NMR data on these phases, obtained in our laboratories, are listed in Table I, with spectra shown in Figure 4.

The ^{15}N spectrum of the La-α-wollastonite phase, $LaSiO_2N$, shows resonances at significantly higher frequency than those of Si_3N_4 or Si_2N_2O. This phase has the α-wollastonite structure with the nitrogen atoms present in three-membered $[Si_3O_6N_3]$ rings,

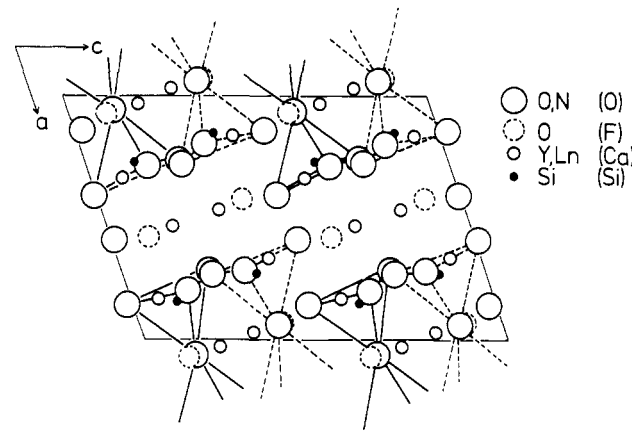

Figure 6. (010) projection of the anticipated atomic distribution in lanthanum N–YAM phase, $La_4Si_2O_7N_2$. Y, Ln indicates yttrium or a lanthanide as appropriate. No detailed crystal structure determination has been carried out on this phase, and the diagram therefore shows the atomic positions in the parent *cuspidine* structure ($Ca_4Si_2O_7F_2$).

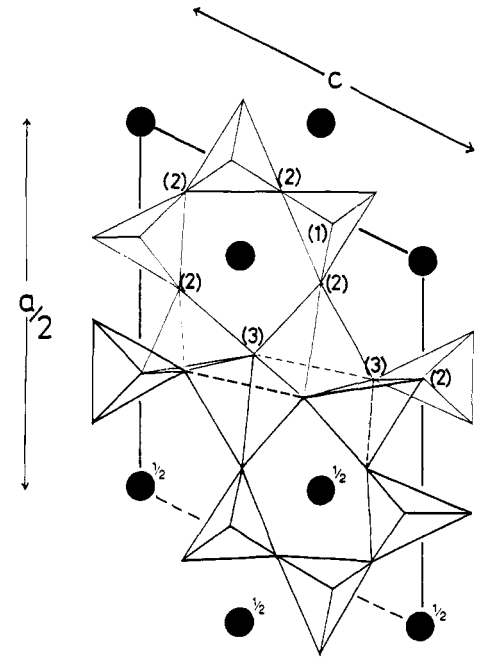

Figure 7. Proposed crystal structure of La "new phase", projected along the y axis. Half the unit cell is shown. N, O sites of the asymmetric unit have their coordination by silicon indicated as 1, 2, or 3.

occupying bridging sites between pairs of Si-centered tetrahedra and also linked to two lanthanum atoms (Figure 5).[33] The nitrogen environment is therefore more ionic than Si_3N_4 or Si_2N_2O.

It was hoped that the La–N–YAM phase (Figure 6), in which N is bonded covalently to only one silicon,[8,9] would also give rise to a characteristic chemical shift, probably at an even more positive value of δ_N. It proved impossible, however, to observe a significant ^{15}N signal from this phase, presumably because of a very long T_1 together with a low nitrogen concentration in the phase.

The so-called "new phase" in the La–Si–O–N system (phase "N" in Figure 3) was originally believed to have a composition $La_2O_3{\cdot}2Si_3N_4$, but recent work has shown that the composition is closer to $La_3Si_8O_4N_{11}$ and a provisional structure has been proposed (Figure 7).[34] Relative to an $La_3Si_8O_4N_{11}$ formula unit, four nitrogens occupy $[NSi_3]$ sites, nine oxygen + nitrogen atoms occupy $[NSi_2]$ sites, and the remaining two nonmetals (believed

(31) Inoue, Z.; Mitomo, M.; Ii, N. *J. Mater. Sci.* **1980**, *15*, 2915.
(32) Mitomo, M.; Izumi, F.; Horiuchi, S.; Matsui, Y. *J. Mater. Sci.* **1982**, *17*, 2359.
(33) Morgan, P. E. D.; Carroll, P. J. *J. Mater. Sci. Lett.* **1977**, *12*, 2243.
(34) Leach, M. J.; Harris, R. K.; Thompson, D. P. Manuscript in preparation.

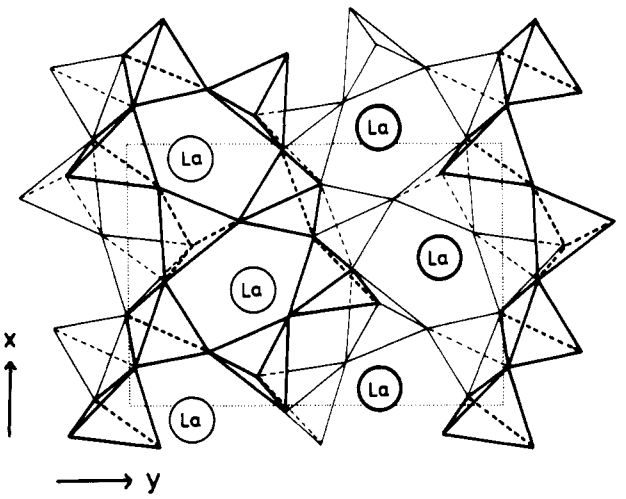

Figure 8. (001) projection of the orthorhombic crystal structure of $LaSi_3N_5$. Bold tetrahedra and lanthanum atoms correspond to sites occupied at heights of one-half along the z axis.

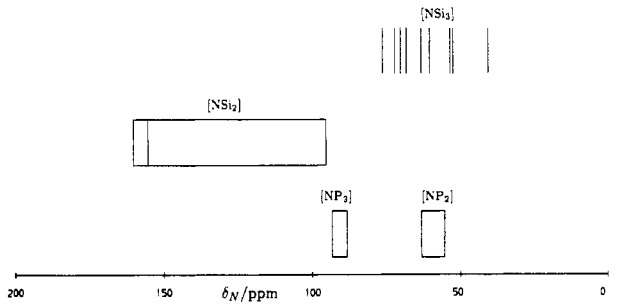

Figure 9. Diagram to show the influence of coordination environment on the ^{15}N chemical shift for La–Si–O–N and nitrogenous sodium phosphate phases.

to be oxygen) are coordinated to one silicon and three lanthanum atoms. The structure (Figure 7) has considerable similarities with $LaSi_3N_5$ (Figure 8), especially in the region of $[NSi_3]$ nitrogen atoms. The ^{15}N NMR spectrum of the "new phase" clearly shows two bands which, by comparison with compounds described above and ^{29}Si NMR data,[9] can be attributed to $[NSi_3]$ and $[NSi_2]$ environments from considerations of both chemical shift and breadth. The intensity ratio of the $[NSi_3]$ and $[NSi_2]$ peaks is consistent with the expected composition, provided the $[NSi_2]$ sites contain N and O in the ratio 3.5:1. It is assumed the monocoordinated sites contain only oxygen, as expected from Pauling's rule.

Isomorphous substitution of Si–N by Al–O is well-known in many sialon ceramics, and the ^{15}N spectrum of an aluminum-substituted "new phase" (approximate composition $La_3Si_6Al_2O_6N_9$) shown in Figure 4d indicates a reduction in $[NSi_2]$ peak intensity relative to $[NSi_3]$, consistent with the expected incorporation of O into more 'ionic' sites.

The spectrum of $LaSi_3N_5$ is surprising. On the basis of the published (but not very detailed) crystal structure (Figure 8) of this compound,[31,35,36] it would be expected that a 3:2 ratio in peak areas would be observed for $[NSi_2]$:$[NSi_3]$ resonances. The observed ratio (4:3) is very close to this, but the shape of the $[NSi_2]$ resonance (see Figure 4) is very complex for a peak resulting from only three crystallographic environments. It is possible that unaveraged (^{15}N, ^{139}La) dipolar coupling is a significant cause of line broadening in this phase. The peak due to $[NSi_3]$ environments is, by contrast, very narrow, as found in other phases containing this environment.

The δ_N values obtained from La–Si–O–N phases are summarised in Figure 9, together with those of Bunker et al.[30] described above. The two different silicon environments, $[NSi_3]$

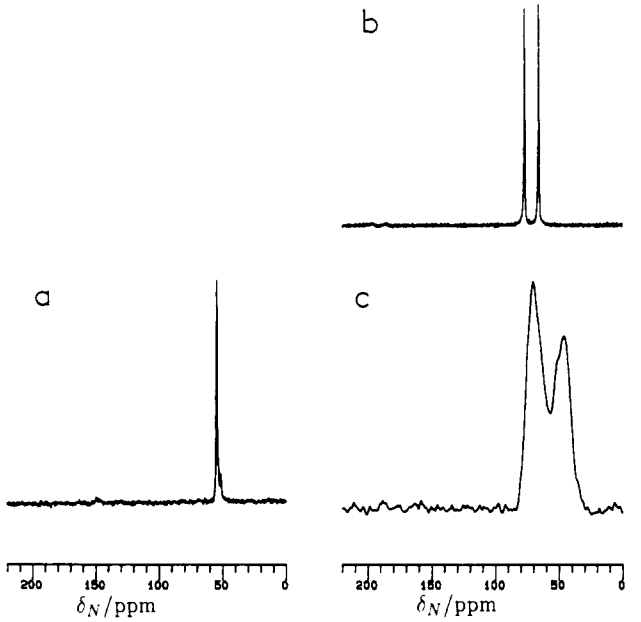

Figure 10. Nitrogen-15 MAS spectra at 30.4 MHz for wurtzite phases: (a) LiSiON, (b) $MgSiN_2$, (c) $MgSiAlN_3$. Spectrometer conditions (each in order a to c): spin rate 2.90, 3.68, 3.50 kHz; pulse angle 24°, 23°, 30°; number of transients 62, 62, 258; recycle delay 300 s in each case. The shoulder to low frequency in a arises from impurity Si_3N_4.

and $[NSi_2]$, give distinctly different chemical shift values. The separation of shifts is found to be much greater than in ^{29}Si NMR for changes in environment,[7-9] as would be expected from consideration of the effect of p-electron density on the paramagnetic contribution to the shielding constant, σ_p. The spread of shifts within each range is also found to be greater than in ^{29}Si NMR. No explanation for the values of δ_N within each range has been proposed.

The results for coordination to silicon contrast with those for coordination to phosphorus. In sodium phosphate glasses, addition of a third phosphorus coordinating atom has a deshielding effect on nitrogen, whereas in the analogous case for coordination by silicon the third atom causes shielding.

Very recently, Kruppa et al.[37] have examined the ^{15}N spectra of a Y–Si–Al–O–N glass and crystallization products. They identify two broad resonances (41 ppm, 87 ppm) in the spectrum of the glass which they assign to $[NSi_3]$ and $[NSi_2]$ environments, respectively, by analogy to the data in refs 19 and 20. The spectrum of the crystallized glass shows peaks assigned to Si_2N_2O (43.2 ppm) and β-Si_3N_4 (52.7 ppm), plus a broad peak centered at 148.5 ppm (probably $YSiO_2N$ or an Al-substituted version). There is also a sharp peak with some structure at 284.9 ppm which cannot be assigned with certainty but which may be due to a nitrogen-substituted YAG phase.

Sjöberg et al.[38] have recently examined β'- and O'-sialons and 21R sialon polytypoid by ^{15}N MAS NMR. The spectra of β'- and O'-sialons are in agreement with those of β-Si_3N_4 and Si_2N_2O referred to above. The spectrum of the polytypoid phase (see also ref 19) cannot be interpreted at present.

Wurtzite Phases. These are a series of Li- and Mg-containing nitrogen ceramic phases with structures which are superlattices of the basic AlN (wurtzite-type) arrangement with nitrogen in four-coordinated environments but cations ordered in different ways depending on the composition.[39] Thus, relative to the basic a_H and c_H dimensions of the hexagonal AlN cell, the orthorhombic superlattice cells are

for $LiSiNO$ and $MgSiN_2$: $a_0 = \sqrt{3}a_H$, $b_0 = 2a_H$, $c_0 = c_H$

for $LiSi_2N_3$ and $MgAlSiN_3$: $a_0 = \sqrt{3}a_H$, $b_0 = 3a_H$, $c_0 = c_H$

(35) Inoue, Z.; Sawada, T.; Ohsumi, K.; Sadanaga, R. *Acta Crystallogr.* **1981**, *A37*, C154.
(36) Inoue, Z. *J. Mater. Sci. Lett.* **1985**, *4*, 656.
(37) Kruppa, D.; Dupree, R.; Lewis, M. H., *Mater. Lett.*, **1991**, *11*, 195.
(38) Sjöberg, J.; Harris, R. K.; Apperley, D. C., *J. Mater. Chem.* in press.
(39) Thompson, D. P. *Mat. Res. For.* **1989**, *47*, 21.

Table II. ^{15}N MAS NMR Data for Wurtzite Phases

phase	δ_N/ppm	fwhh/Hz	intensity
LiSiON	54.4	25	
$MgSiN_2$	65.5	25	1
	76.7	25	1
$MgSiAlN_3$	45.0	500	3
	70.2	500	4

Whereas $LiSi_2N_3$ and $MgAlSiN_3$ have identical structures in space group $Cmc2_1$ (because Al and Si are apparently disordered in 8(b) sites), the preferential ordering of O round Li and N round Si in LiSiNO results in different space groups for LiSiNO ($Pca2_1$) and $MgSiN_2$ ($Pna2_1$). Marshall et al.[26] have reported a δ_N value for AlN of 64 ppm from an unenriched sample. The other wurtzite phases discussed above have been examined by ^{15}N MAS NMR on enriched samples. Spectra are shown in Figure 10, with data listed in Table II. All of the chemical shifts for nitrogen in these wurtzite phases lie in the narrow range 45–77 ppm, essentially the same range as for $[NSi_3]$ coordination outlined in Figure 9.

$MgSiN_2$ gives two very narrow resonances with a 1:1 intensity ratio. This corresponds with the crystal structure,[40,41] in which nitrogen is present in two distinct $[NSi_2Mg_2]$ environments. Again, δ_N is seen to be extremely sensitive to changes in crystallographic environment. The resonances are very narrow, indicating a high degree of crystalline order. LiSiON gives a single resonance (again in agreement with the known crystal structure[42]), assigned to a $[NSi_3Li]$ environment. $MgSiAlN_3$ gives a spectrum which is difficult to account for, even in conjunction with the ^{29}Si and ^{27}Al spectra.[10,19] The crystal structure of the phase has been determined,[43] although the Si/Al ordering scheme (if any) is not known. The nitrogen environments present are $[NMg_2(Si,Al)_2]$ and $[NMg(Si,Al)_3]$, and the most likely explanation of the ^{15}N spectrum is that the two peaks observed are due to these two types of environments, with Si/Al ordering affecting only line widths, but other explanations are possible.

All of the above spectra seem to indicate that nitrogen in tetrahedral (sp^3) and planar (sp^2) covalent coordination environments give rise to essentially indistinguishable chemical shifts, which are far removed from those from $[NSi_2]$ environments, in which N is also coordinated to basically ionic moieties. This implies that electron densities on the sp^2 and sp^3 nitrogens in covalent structures are very similar and confirms that Li and Mg bond covalently in these phases.

It is thus concluded that δ_N provides an excellent measure of the degree of ionicity in solid-state systems, as found in solution.[24]

Oxygen-17 NMR. As with nitrogen-15, the low isotopic abundance of the oxygen-17 nucleus (0.037%) makes isotopic enrichment almost essential for solid-state NMR studies. In other ways ^{17}O is a relatively favorable NMR nucleus, with $I = {}^5/_2$, a moderate magnetic moment, and a small electric quadrupole moment (about one-sixth that of ^{27}Al). Samples enriched in ^{17}O should thus give spectra with acceptably narrow lines. In most cases, only the $({}^1/_2 \leftrightarrow {}^{-1}/_2)$ transition is observed, broadened principally by second-order quadrupolar coupling. Three types of inorganic systems will be considered in this review: metal oxides, silicates and zeolites, and nitrogen ceramics.

Metal Oxides. A wide range of metal oxides has been examined by ^{17}O MAS NMR, the vast majority on enriched samples. The group IIa metal oxides, MO, were examined by Schramm et al.[44] and Turner et al.[45] δ_0 was found to lie in the range 26 (BeO) to 629 ppm (BaO) and could be correlated accurately with the cube of the metal ionic radius ($r_{2+}{}^3$). Quadrupole coupling constants, χ_Q, are all small (0–20 kHz), as expected from the high symmetry of the oxygen sites in these phases. In group IIb metal oxides,[45] δ_0 can again be correlated with $r_{2+}{}^3$, although with different correlation coefficients. Values of χ_Q are much greater in these phases, in agreement with an increase in oxygen asymmetry as the phases become more covalent.

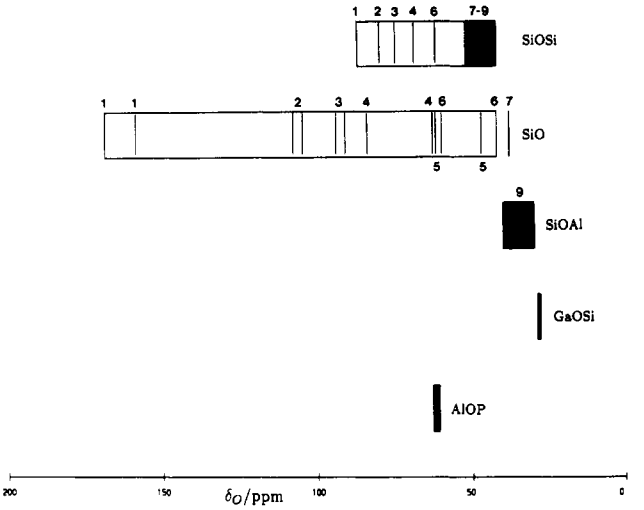

Figure 11. Diagram to show the variation of ^{17}O chemical shifts in silicates and zeolites. The numbers refer as follows: 1 = $BaSiO_3$, 2 = $SrSiO_3$, 3 = $CaSiO_3$, 4 = $CaMgSi_2O_6$, 5 = Mg_2SiO_4, 6 = $MgSiO_3$, 7 = glass, 8 = SiO_2, 9 = zeolites.

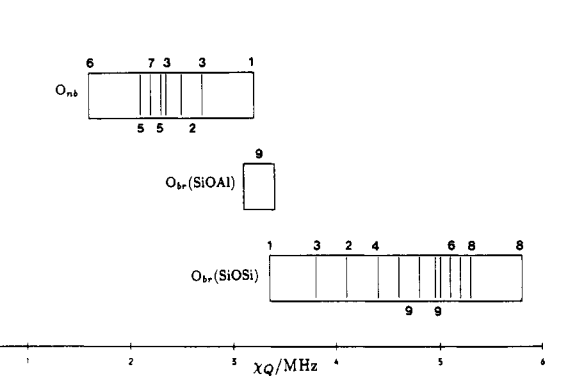

Figure 12. Summary of ^{17}O quadrupole coupling constants in silicates and zeolites. The numbers refer as in the caption to Figure 8 with, in addition, 10 = Al_2O_3/AlOOH.

Walter and Oldfield[46] have examined a series of aluminum oxides and hydroxides. The possible oxygen environments, $[OAl_4]$ and $[Al_2OH]$, can be distinguished by both chemical shift (70–75 ppm for $[OAl_4]$ and 40 ppm for $[Al_2OH]$) and quadrupole coupling constant (1.2–2.2 MHz for $[OAl_4]$ and 5–6 MHz for $[Al_2OH]$).

Yang et al.[47] have obtained the ^{17}O spectra of Tl_2O_3, Bi_2O_3, Y_2O_3, and BaO_2. Chemical shifts lie in the range 200–370 ppm. In a very recent natural-abundance study Bastow and Stuart[48] have studied a range of metal oxides. The oxygen chemical shift is correlated with the fluorine shift in the corresponding fluorides, but no explanation of this observation was proposed.

Comparison of all of the data above indicates that δ_0 can be correlated with the ionic radius of the metal ion in metal oxides. No explanation of this effect has been proposed, and it will be discussed again in a later section of this paper.

Silicates and Zeolites. Oxygen-17 resonances from silicates and zeolites tend to be much broader than from metal oxide systems: oxygen environments are in general much more covalent

(40) Wild, S.; Grievson, P.; Jack, K. H. *Spec. Ceram.* **1972**, *5*, 289.
(41) David, J.; Laurent, Y.; Lang, J. *Bull. Soc. Fr. Miner. Cristallogr.* **1970**, *93*, 153.
(42) Laurent, Y.; Guyader, J.; Roult, G. *Acta Crystallogr.* **1981**, *B37*, 911.
(43) Perera, D.S. Ph.D. Thesis, University of Newcastle upon Tyne, 1976.
(44) Schramm, S.; Kirkpatrick, R. J., Oldfield, E. *J. Am. Chem. Soc.* **1983**, *105*, 2483.
(45) Turner, G. L.; Chung, S. E.; Oldfield, E. *J. Magn. Reson.* **1985**, *64*, 316.
(46) Walter, T. H.; Oldfield, E. *J. Phys. Chem.* **1989**, *93*, 6744.
(47) Yang, S.; Park, K. D.; Oldfield, E. *J. Am. Chem. Soc.* **1989**, *111*, 7278.
(48) Bastow, T. A.; Stuart, S. N. *Chem. Phys.* **1990**, *143*, 459.

Table III. ^{17}O MAS NMR Data for La-Si-Al-O-N Phases

phase	27.1 MHz δ^*_0/ppm	27.1 MHz fwhh/Hz	40.7 MHz δ^*_0/ppm	40.7 MHz fwhh/Hz	corrected δ_0[e]/ppm	corrected $\lvert\chi_Q\rvert$[f]/MHz	assignment
La-N-wollastonite,[c] $LaSiO_2N$	170	1700	195	1600	215	2.4	SiO nonbridging
La-N-YAM,[c] $La_4Si_2O_7N_2$	575	950	575	1100	575	~0	"ionic"
	175	2000	200	1700	220	2.4	SiO nonbridging
La-Al-N-YAM,[c] La_4SiAlO_8N	573	1000	570	1000	570	~0	"ionic"
	286	1500	300	2000	311	1.8	AlO nonbridging
	169	1600	212	2000	246	3.1	SiO nonbridging
La-N-apatite, $La_{10}Si_6O_{24}N_2$	*a*		596	1000	(596)	*b*	"ionic"
	153	1600	170		184	1.9	SiO nonbridging
					219?[d]		SiO nonbridging

[a] No peak observed at 27.1 MHz, so the error in the corrected δ_0 is large. [b] <1 MHz, as estimated from line width. [c] Bridging oxygen resonance not observed (the position is probably occupied by nitrogen). [d] Shoulder; presumably SiO_3N oxygens. [e] ±5 ppm. [f] Possible errors substantial (see the text).

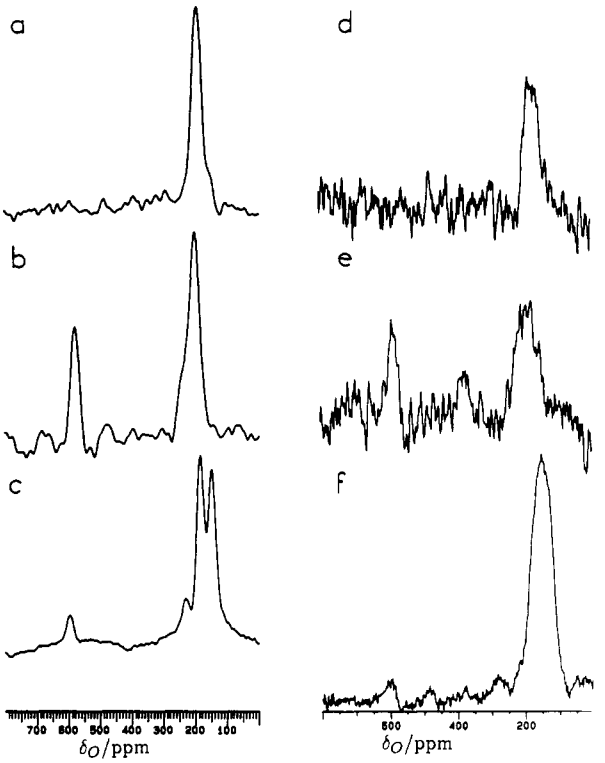

Figure 13. Oxygen-17 MAS spectra at 40.7 MHz (a–c) and 27.1 MHz (d–f) for isotopically enriched La-Si-Al-O-N phases: (a) and (d) La-N-wollastonite, $LaSiO_2N$, (b) and (e) La-N-YAM, $La_4Si_2O_7N_2$, (c) and (f) La-N-apatite, $La_{10}Si_6O_{24}N_2$. Spectrometer conditions (each in order a–f): spin rate 4.10, 4.15, 8.00, 3.01, 3.00, 300 kHz; pulse angle 10°, 10°, 23°, 23°, 23°, 23°; number of transients 1200, 1200, 6000, 600, 800, 6700; recycle delay 2, 2, 1, 5, 5, 1 s.

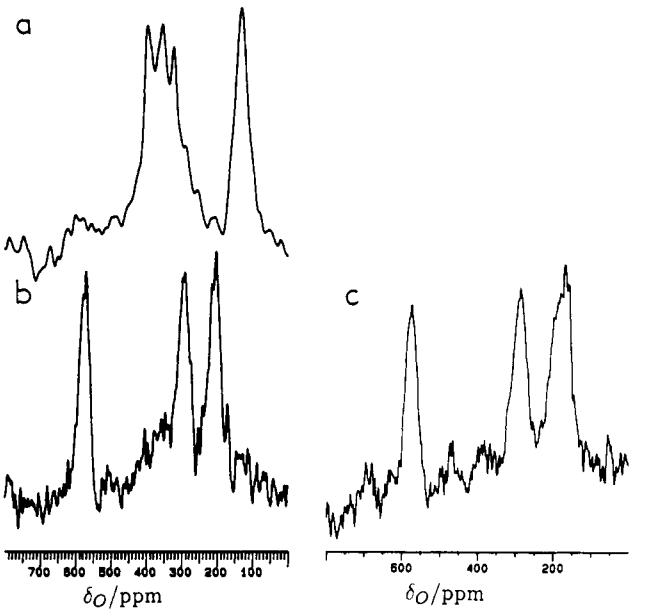

Figure 14. Oxygen-17 MAS spectra of isotopically enriched (a) N-YAM, $Y_4Si_2O_7N_2$, (b) and (c) La-Al-N-YAM, La_4SiAlO_8N. Spectrometer conditions: for a and b, frequency 40.7 MHz, spin rate 8.00 and 8.90 kHz, respectively, pulse angle 15°, number of transients 55000 and 2000, respectively, recycle delay 1 s. For c frequency 27.1 MHz, spin rate 3.03 kHz, pulse angle 23°, number of transients 600, recycle delay 5 s.

and asymmetric. Typical values of χ_Q in silicates lie in the region 1–5 MHz. MAS NMR has been successfully used to minimize broadening due to second-order quadrupolar coupling,[49] and, more recently, dynamic-angle and double-rotation techniques have successfully applied to narrow ^{17}O resonances in silicates.[50]

The observed chemical shift range for ^{17}O in silicates is around 100 ppm, but unfortunately substantial band overlap occurs, making extraction of accurate NMR parameters difficult. Shift data from a range of studies are summarized in Figure 11.[47,49,51–55]

Within these ranges correlations with other variables have been suggested. Timken et al.[51] have shown that δ_0 can be correlated with counterion radius in the $MSiO_3$ phases, in a manner analogous to that for the metal oxides. The effect of cation radius is greater (r_{2+}^2) for nonbridging oxygens, which are in more ionic environments, than for bridging oxygens ($r_{2+}^{1/2}$). It is clear from these results that a great deal can be learnt about oxygen environment from studies of isostructural series. For small cations, it is shown that δ_0 values alone are not sufficient to distinguish bridging and nonbridging oxygen environments.

Rough correlation of χ_Q with oxygen coordination (Figure 12) shows that the value of χ_Q can provide a valuable indication of oxygen environment. It is also possible to make quantitative correlations. Timken et al.[51] have found a good correlation between χ_Q and cation electronegativity for the O_{br} and O_{nb} (bridging and nonbridging oxygens) sites in the $MSiO_3$ metasilicates. Janes and Oldfield[56] have attempted to calculate χ_Q (and η_Q) from considerations of the oxygen valence-bond orbital asymmetry using a Townes–Dailey approach, with good agreement (±20%) for SiO_2 and diopside. Timken et al.[54] have performed similar calculations on zeolites.

(49) Schramm, S.; Oldfield, E. *J. Am. Chem. Soc.* **1984**, *106*, 2502.
(50) Mueller, K. T.; Wu, Y.; Chmelka, B. F.; Stebbins, J.; Pines, A. *J. Am. Chem. Soc.* **1991**, *113*, 32.
(51) Timken, H. K. C.; Schramm, S. E.; Kirkpatrick, R. J.; Oldfield, E. *J. Phys. Chem.* **1987**, *91*, 1054.
(52) Bunker, B. C.; Tallant, D. R.; Kirkpatrick, R. J.; Turner, G. L. *Phys. Chem. Glasses* **1990**, *31*, 30.
(53) Timken, H. K. C.; Turner, G. L.; Gilson, J. P.; Welsh, L. B.; Oldfield, E. *J. Am. Chem. Soc.* **1986**, *108*, 7231.
(54) Timken, H. K. C.; Janes, N.; Turner, G. L.; Lambert, S. L.; Walsh, L. B.; Oldfield, E. *J. Am. Chem. Soc.* **1986**, *108*, 7236.
(55) Kirkpatrick, R. J.; Dunn, T.; Schramm, S.; Smith, K. A.; Oestrike, R.; Turner, G.; *Structure and Bonding in Non-Crystalline Solids*; Walrafer and Reeves, 1986; p 303.
(56) Janes, N.; Oldfield, E. *J. Am. Chem. Soc.* **1986**, *108*, 5743.

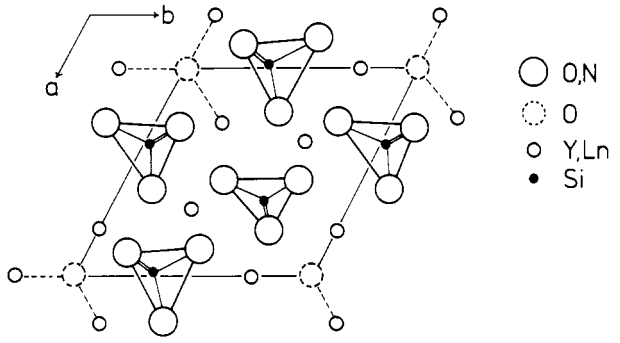

Figure 15. (001) projection of the lower half of the hexagonal unit cell relevant to lanthanum apatite, $La_{10}(SiO_4)_6N_2$. Y, Ln indicates yttrium or a lanthanide as appropriate.

Y–Si–O–N and La–Si–O–N Phases. Oxygen-17 data, obtained at 27.1 and 40.7 MHz in our laboratories, on La–Si–Al–O–N phases are listed in Table III, including corrected oxygen chemical shifts and quadrupolar coupling constants calculated from the change in apparent chemical shift.[1] Given the difficulties of referencing, location of band centres and use of only two magnetic fields, the shift corrections and quadrupolar data must be regarded as only ballpark estimates. However, it does seem clear that "ionic" oxygen sites have very low quadrupolar coupling constants. Spectra are illustrated in Figures 13 and 14, including also the spectrum of yttrium N–YAM, which is isostructural with the lanthanum phase. There are many unresolved issues in these spectra, but the following conclusions can nevertheless be drawn.

(i) La–N–wollastonite: Spectra from both spectrometers show a single peak. All the oxygen atoms in the structure (Figure 5) occupy nonbridging sites in the $Si_3O_6N_3$ three-membered rings, and the chemical shift and quadrupolar coupling constant are fully consistent with similar environments in metal silicates (vide supra). Notably, $LaSiO_2N$ and $BaSiO_3$ are isoelectronic and give very similar nonbridging oxygen peaks. However, the peak for N–wollastonite is somewhat sharper than expected from the value of χ_Q deduced from the shift changes (see Table III).

(ii) La–N–YAM: The structure of this phase is similar to that of cuspidine, $Ca_4Si_2O_7F_2$, and the $M_4Al_2O_9$ aluminates (M = Y, Ln), and consists of $Si_2O_5N_2$ groups joined together by La_4O units (see Figure 6). Oxygen-17 spectra unambiguously show the presence of two distinct resonances: δ_0 = 575 ppm, $\chi_Q \sim 0$ MHz and δ_0 = 220 ppm, χ_Q = 2.4 MHz. There also seems to be a third peak in the spectrum obtained at 27.1 MHz, the origin of which is not clear. There may also be a high-frequency shoulder on the band at 220 ppm in the 40.7 MHz spectrum. The first peak is assigned to oxygen bonded directly to four La^{3+} (i.e., "ionic" oxygen), by analogy to the spectra of La_2O_3 (δ_0 = 584 ppm[48]) and BaO (δ_0 = 629 ppm[45]). The low χ_Q value also implies a relatively symmetric environment. The second peak is assigned to nonbridging oxygen by comparison with the spectra of $LaSiO_2N$ above, there presumably being insufficient resolution to distinguish $-SiO_3$ and $-SiO_2N$ sites. The resonance from bridging oxygen, which would be expected at $\delta_0 = \sim 85$ ppm, $\chi_Q \sim 4$ MHz by comparison with data from silicates, is not observed. It may be broadened by second-order quadrupolar coupling and other interactions to such an extent that it cannot be distinguished from background or perhaps only nitrogen occupies bridging positions. Dupree et al.[7] claim (from ^{29}Si spectra) that nitrogen is entirely nonbridging in N–YAM and cite a somewhat cryptic note[57] giving neutron diffraction results in support. It is unfortunate that we were unable to obtain a suitable ^{15}N spectrum of La–N–YAM (Figure 4b), but it needs to be pointed out that the factors influencing ^{29}Si shifts are complex and it is not impossible, albeit unlikely, for SiO_2N_2 and SiO_3N groups (such as would be contained in a nitrogen-bridged $Si_2N_2O_5$ unit) to give indistinguishable resonances.

(iii) La N–apatite (Figure 15) contains oxygen in O_{nb} environments (in SiO_4 and SiO_3N units in the ratio 16:6) and an ionic environment, in which oxygen is located on a C_3 axis and is coordinated to three identical lanthanums. The latter gives a clear signal at 596 ppm in the 40.7-MHz spectrum. There is a complex band in the region 100–250 ppm, for which the interpretation must be regarded as tentative. The two most intense peaks may result from second-order quadrupolar effects on the SiO_4 signal, the splitting being of the order of magnitude expected for the parameters given in Table III (though corresponding to a larger quadrupole coupling constant, ca. 2.8 MHz). The shoulder at 219 ppm may arise from the SiO_3N oxygens. Alternatively, the two peaks may arise from the two different oxygen sites, though the intensity ratio is not consistent with this assignment unless impurity material is present (which is unlikely).

(iv) The spectrum of the yttrium N–YAM is surprising. The complex series of peaks in the region 350–400 ppm is clearly due to $[OY_4]$ ionic environments. These peaks are shifted to substantially lower frequency in comparison with the lanthanum analogue. The band may be complicated by second-order quadrupolar effects, though these are not visibly present for La–N–Y–YAM, and they are intrinsically unlikely for an "ionic" oxygen site with 4-fold coordination.

(v) The spectrum for La–Al–N–YAM shows three clear signals at both applied fields. These can be easily assigned to ionic, AlO_4 and nonbridging SiO_3N oxygens (from high to low frequency). Once more, no bridging oxygen signals can be detected, so that either these are too broad to observe or the bridging sites are entirely occupied by nitrogen. The value of χ_Q deduced from the shift dependence on magnetic field seems too large, given that no quadrupolar splitting is seen.

Discussion of ^{17}O and ^{15}N Chemical Shifts. Oxygen-17 chemical shifts in the M–Si–O–N phases are found to follow trends similar to those in the metal silicates. In general, increasing coordination to large ions leads to a high-frequency shift. This allows ready distinctions of nonbridging and ionic oxygen sites. Similar trends are also seen in ^{15}N shifts from the same phases.

No explanation for the increase in δ_0 with coordination to large ions has been proposed. It has been pointed out[45] that the trend is not directly related to cation electronegativity. We propose that δ_0 (and δ_N) in silicates and nitrogen ceramics can, however, be related to ion polarizability rather than electronegativity. An oxygen atom in the vicinity of more polarizable (i.e., larger) cations can accommodate a larger electron density. If shielding is determined principally by the paramagnetic contribution (as expected for ^{17}O), then increasing electron density will normally cause the chemical shift to increase, as is the case for ^{29}Si (e.g., the change from $[SiO_4]$ to $[SiN_4]$ environments affecting δ_{Si}—see ref 1). Thus increasing the radius of the cation has the effect of also increasing δ_0. This hypothesis is supported by the literature evidence that δ_0 increases more slowly with r_{2+}^3 of the metal in the group IIb metal oxides in comparison with the corresponding group IIa oxides. The effect is most notable in the case where oxygen is bonded principally to large ions (e.g., O^{2-} sites) in comparison to cases where coordination is partially to Si (e.g., O_{nb} sites). O_{br} sites are expected to give the smallest cation-dependent shifts, as found in metal silicates. Cation identity would also be expected to alter χ_Q for ^{17}O, but the lack of suitable high-quality data on nitrogen ceramics has cautioned us against drawing conclusions on this matter yet.

Concluding Remarks

^{17}O and ^{15}N NMR are shown to be of great use in increasing the understanding of the structures of inorganic silicate and nitrogen ceramic phases. In one case, the ^{15}N NMR spectrum aided critically in the determination of the structure of a previously uncharacterized lanthanum silicon oxynitride. The ionicity of the nitrogen or oxygen bonds is found to be the most important factor in determining the chemical shift, and this can be used to distinguish environments in many phases: e.g., $[NSi_2]$ vs $[NSi_3]$ and O_{nb} vs O^{2-}. In ^{17}O NMR, δ_0 is related to the ionic radius of the counterion, and this can be related to cation polarizability and therefore ionicity. However, the quality of ^{17}O spectra is still not fully satisfactory, and some of the outstanding difficulties of interpretation may be overcome

(57) Roult, G.; Bacher, P.; Liebaut, C.; Marchand, R.; Goursat, P.; Laurent, Y. *Acta Crystallogr. (Suppl.)* **1984**, *A40*, C226.

by experiments at still higher magnetic field (which we are currently attempting).

Acknowledgment. We are grateful to the U.K. Science and Engineering Research Council for the award of an Earmarked Studentship to one of us (M.J.L.) under the 21st Century Materials Initiative and for the use of the National Solid-State NMR Service at Durham. We thank R. Dupree for helpful discussions and for information in advance of publication.

Articles

Observation of Heterogeneous Trace (0.4% w/w) Water Uptake in Bisphenol A Polycarbonate by NMR Imaging

Colin A. Fyfe,* Leslie H. Randall, and Nick E. Burlinson

Department of Chemistry, University of British Columbia, Vancouver, British Columbia, V6T 1Y6 Canada

Received May 10, 1991. Revised Manuscript Received December 12, 1991

The uptake of water by injection-molded bars of bisphenol A polycarbonate (Lexan 121 resin) has been monitored by a combination of one-dimensional proton NMR spectroscopy, relaxation time (T_1 and T_2) measurements, and microscopic imaging techniques. The bulk of the water absorbed in the initial stages (20–24 h) of 100 °C water exposure is uniformly distributed throughout the polymer with a trace amount of the water found in clusters of 200–300 μm in size. The water that has aggregated to form these clusters is more mobile, having a T_2 relaxation time 20 times longer than that found for the uniformly distributed water. At longer exposure times (30–40 days) the number of clusters is observed to increase. Although the total amount of water adsorbed is considerably less than 1% w/w, good-quality images are obtained, demonstrating that the NMR microimaging technique can successfully monitor even trace levels of solvent if the molecules are relatively mobile.

Introduction

Bulk polymers are permeable substances, subject to the diffusion of small molecules which can affect their physical and mechanical properties and can result in the degradation of the polymeric material. The recent development of NMR microscopic imaging has provided researchers with a noninvasive way of examining the spatial distribution of absorbed fluids in polymers.[1-6] However, the real advantage of NMR spectroscopy over other methods is its ability to obtain chemical information about the nature and mobility of these absorbed species. In this paper, we wish to report the results of a systematic study in which the one-dimensional ^{1}H NMR spectra, the relaxation parameters of the components and the spatial distribution of water absorbed into injection molded bisphenol A polycarbonate bars were obtained. This particular system is of interest because of the importance of polycarbonate as the material of choice in optical storage systems where it has been suspected that water adsorption may be the critical physical process limiting its performance.[7-9]

Experimental Section

Materials. The polycarbonate sample studies was General Electric Lexan 121 resin which was received as injection-molded izod bars (7 mm × 12 mm cross section). The bars were cut to a cross section of 6 mm × 7 mm and a length of 2 cm from the original 10 cm length. Distilled water was used in the study, and deuterium oxide (99.9 atom % D) was used as received from MSD isotopes.

Gravimetric Analysis. In the present study, polycarbonate pieces 2 cm × 6 mm × 7 mm were immersed in distilled water at 100 °C for up to 40 days, removed periodically, and dried of excess water. The sample was weighed, temporarily sealed in 10-mm-o.d. thin-walled glass NMR tubes, and then subsequently imaged. The sample was then replaced in the water bath after imaging. The limiting amount of water absorbed by the polycarbonate rods was typically <0.80% (w/w). Experiments involving the use of deuterium oxide were carried out in a similar apparatus under a blanket of dry nitrogen gas.

Spectroscopy. NMR measurements were made on a Bruker MSL 400 spectrometer equipped with a microimaging system. All experiments were performed using the proton microimaging probe supplied except that the probehead was modified by replacing the vertical saddle coil with an 11-mm horizontal solenoid coil that was demonstrated to have superior S/N and rf homogeneity characteristics. The nonselective 90° and 180° rf pulses were 9 and 18 μs, respectively. Quadrature phase cycling was used in all spectroscopic measurements.

One-dimensional ^{1}H NMR spectra were obtained by the standard one pulse method and by the Carr–Purcell spin–echo experiment.[10] The Carr–Purcell sequence with the modification of alternating the phase of the 180° pulses as developed by

(1) Blackband, S.; Mansfield, P. *J. Phys. C: Solid State Phys.* **1986**, *19*, L49.
(2) Rothwell, W. P.; Holeck, P. R.; Kershaw, J. A. *J. Polym. Sci., Polym. Lett. Ed.* **1984**, *22*, 241.
(3) Weisenberger, L. A.; Koenig, J. L. *Appl. Spectrosc.* **1989**, *43*, 1117.
(4) Hoh, K.-P.; Perry, B.; Rotter, G.; Ishida, H.; Koenig, J. L. *J. Adhesion* **1989**, *27*, 245.
(5) Weisenberger, L. A.; Koenig, J. L. *Macromolecules* **1990**, *23*, 2445.
(6) Tabak, F.; Corti, M. *J. Chem. Phys.* **1990**, *92*, 2673.
(7) Schilling, F. C.; Ringo, W. M.; Sloane, N. J. A. Bovey, F. A. *Macromolecules* **1981**, *14*, 532.
(8) Bair, H. E.; Johnson, G. E.; Merriweather, R. *J. Appl. Phys.* **1978**, *49*, 4976.
(9) Pryde, C. A.; Kelleher, P. G.; Hellman, M. Y.; Wentz, R. P. *Polym. Eng. Sci.* **1982**, *23*, 370.
(10) Carr, H. Y.; Purcell, E. M. *Phys. Rev.* **1954**, *94*, 630.

0897-4756/92/2804-0267$03.00/0